Meteorologische Zeitschrift, Vol. 25, No. 3, 267–279 (published online March 21, 2016)

Mettools IX

Impact of meteorological conditions on airborne fine particle composition and secondary pollutant characteristics in urban area during winter-time

Klaus Schäfer[1*], Michael Elsasser[2,3,4], Jose M. Arteaga-Salas[1,8], Jianwei Gu[2], Mike Pitz[2,6], Jürgen Schnelle-Kreis[2,8], Josef Cyrys[2], Stefan Emeis[1], Andre S.H. Prévôt[7] and Ralf Zimmermann[2,3]

[1]Karlsruhe Institute of Technology (KIT), Institute of Meteorology and Climate Research, Department of Atmospheric Environmental Research (IMK-IFU), Garmisch-Partenkirchen, Germany
[2]Helmholtz Zentrum München, German Research Centre for Environmental Health (HMGU), Joint Mass Spectrometry Centre, Neuherberg Germany;
[3]University of Rostock, Institute of Chemistry, Joint Mass Spectrometry Center, Rostock, Germany
[4]Current affiliation: Deutscher Wetterdienst, Meteorological Observatory, Hohenpeissenberg, Germany
[5]Helmholtz Zentrum München, German Research Center for Environmental Health (HMGU), Institute of Epidemiology II (EPI 2), Neuherberg, Germany
[6]Current affiliation: Bavarian Environment Agency, Augsburg, Germany
[7]Paul Scherrer Institute (PSI), Laboratory of Atmospheric Chemistry, Villigen, Switzerland
[8]HICE – Helmholtz Virtual Institute of Complex Molecular Systems in Environmental Health: Aerosols and Health, Munich, Germany

(Manuscript received March 24, 2015; in revised form October 6, 2015; accepted November 9, 2015)

Abstract

The assessment of airborne fine particle composition and secondary pollutant characteristics in the case of Augsburg, Germany, during winter (31 January–12 March 2010) is studied on the basis of aerosol mass spectrometry (3 non-refractory components and organic matter, 3 positive matrix factorizations (PMF) factors), particle size distributions (PSD, 5 size modes, 5 PMF factors), further air pollutant mass concentrations (7 gases and VOC, black carbon, PM_{10}, $PM_{2.5}$) and meteorological measurements, including mixing layer height (MLH), with one-hourly temporal resolution. Data were subjectively assigned to 10 temporal phases which are characterised by different meteorological influences and air pollutant concentrations. In each phase hierarchical clustering analysis with the Ward method was applied to the correlations of air pollutants, PM components, PM source contributions and PSD modes and correlations of these data with all meteorological parameters. This analysis resulted in different degrees of sensitivities of these air pollutant data to single meteorological parameters. It is generally found that wind speed (negatively), MLH (negatively), relative humidity (positively) and wind direction influence primary pollutant and accumulation mode particle (size range 100–500 nm) concentrations. Temperature (negatively), absolute humidity (negatively) and also relative humidity (positively) are relevant for secondary compounds of PM and particle ($PM_{2.5}$, PM_{10}) mass concentrations. NO, nucleation and Aitken mode particle and the fresh traffic aerosol concentrations are only weakly dependent on meteorological parameters and thus are driven by emissions. These daily variation data analyses provide new, detailed meteorological influences on air pollutant data with the focus on fine particle composition and secondary pollutant characteristics and can explain major parts of certain PM component and gaseous pollutant exposure.

Keywords: airborne particle composition, airborne particle size distribution, aerosol mass spectrometry, air pollutants, meteorological parameters, mixing layer height, hierarchical clustering

1 Introduction

Particulate matter (PM) and especially ultrafine particles (UFP, aerodynamic diameters < 100 nm) are of a high health risk (Rückerl et al., 2011) as particles of smallest diameter penetrate deepest into the lungs, contribute to reduced lung function (Wu et al., 2013) and can be transported to the organs via the bloodstream. It is important from the point of view of health protection to know not only the chemical composition and emission sources, but also the meteorological influences upon the particle mass concentration (PMC), particle number concentration (PNC), different particle size fractions as well as the particle chemical composition.

Urban regions are frequently affected by enhanced air pollution and limit value exceedances of PM_{10} (par-

*Corresponding author: Klaus Schäfer, Karlsruhe Institute of Technology (KIT), Institute of Meteorology and Climate Research, Department of Atmospheric Environmental Research (IMK-IFU), Kreuzeckbahnstr. 19, 82467 Garmisch-Partenkirchen, Germany, e-mail:klaus.schaefer@kit.edu

DOI 10.1127/metz/2016/0684

Gebrüder Borntraeger Science Publishers, Stuttgart, www.borntraeger-cramer.com

ticles with aerodynamic diameters < 10 µm, 24-hour average PM_{10} of 50 µg/m^3 should not to be exceeded more than 35 times in the European Union in any calendar year) and NO_2 (hourly limit value of 200 µg/m^3 should not to be exceeded more than 18 times in any calendar year) according to Directive 2008/50/EC (2008). Not only emissions and chemical transformation processes but also wind speed, wind direction and mixing layer height (MLH) impact air pollutant concentrations, because these are important factors for exchange processes of air pollutants and for particle size distributions (PSD) (Schäfer et al., 2006, 2011; Alföldy et al., 2007; Barmpadimos et al., 2011, 2012). Further, temperature and humidity influence secondary gas and particle formation and particle hygroscopic growth (see e.g. Malm and Day, 2001).

A study of wintertime particle composition and source apportionment of the organic fraction was performed in 2010 in the metropolitan area of Paris, France (Crippa et al., 2013). It was found that the dominant primary sources of PM were traffic, biomass burning and cooking. The secondary organic aerosol (SOA) contributed more than 50 % to the total organic mass and included a highly oxidized factor which was related to diverse sources including wood burning emissions. While it was concluded that particulate pollution in Paris was dominated by regional factors, meteorological impacts were not discussed in detail. The meteorological influences upon air quality were investigated already by Rost et al. (2009) and Pal et al. (2014) for temporal variation of PM_{10} and Tai et al. (2010) for daily-mean $PM_{2.5}$ mass concentrations, but not for PM components and gaseous pollutants, Bukowiecki et al. (2003), Wen and Yeh (2010) as well as Xu et al. (2011) for daily variations of air pollutants, but not for PM components, Wu et al. (2013) and Spindler et al. (2013) for daily-mean values, Tandon et al. (2010) for eight-hourly mean data and Elminir (2005) for monthly-mean data only. Tai et al. (2010) and Tandon et al. (2010) stated that up to 50 % of the particulate mass concentration variability can be explained with temperature, relative humidity, precipitation, and circulation (wind and MLH). Bukowiecki et al. (2003) found significantly smaller spatial (urban vs. rural) PNC variation than day-to-day and seasonal variation, while it was more similar only for CO.

Here, the impacts of meteorological conditions are investigated in order to get a deeper understanding of processes directing not only PMC, PNC and thus PSD (transport and dilution) but also secondary particle formation and thus particle composition. The motivation of this study is from the strong temporal variations of gaseous pollutants mass concentrations, PM composition and PM source contributions which cannot be caused by emissions.

The study was performed in the urban area of Augsburg, Germany during a highly polluted winter episode in 2010 with many limit value exceedances. To investigate the assessment of airborne particle composition and secondary pollutant characteristics an urban area like Augsburg provides a lot of emissions sources including industry. During winter-time with stagnant weather conditions the meteorological influences on airborne particle composition, PSD and secondary pollutant characteristics are more important than during other seasons. High temporal resolution (one hour) data is used to study the local as well as the regional scale processes, which are of different temporal variation during the day. The main focus is on organic and ionic PM composition and PM sources (from source apportionment analysis), and thus to assess air pollution exposure.

Particle hygroscopic growth and secondary particle formation are believed to depend on relative humidity (Malm and Day, 2001; Yue et al., 2009; Wen and Yeh, 2010, Zhang et al., 2010; Zhao et al., 2011; Donateo et al., 2012; El-Metwally and Alfaro, 2013; Liu et al., 2013; Wu et al., 2013, Ji et al., 2014). As the gas-phase chemistry is influenced by absolute humidity (Malm and Day, 2001; Liu et al., 2013), it will also be considered along with relative humidity.

Further, MLH which is relevant for the analyses of daily air pollutant variation is monitored by remote sensing with ceilometers and a Radio Acoustic Sounding System (RASS) (see Emeis et al., 2004, 2008; Helmis et al., 2012). In the case of Augsburg, the MLH is much lower in winter (often below 500 m) than in summer (often 1500 to 2300 m) as shown by Emeis et al. (2012). During winter, the MLH determines the near-surface mass concentration of gaseous pollutants and PSD by up to 50 % in areas that are not influenced by strong emissions and during time periods without strong vertical mixing and advection (Schäfer et al., 2006, 2011). But also near major traffic roads air pollutant mass concentrations are influenced by MLH, namely the maximum mass concentrations (Wagner, 2014).

Several correlation analyses are applied for the experimental data to show the impact of dilution and transport (wind speed), mixing volume (MLH), particle growth (humidity), and secondary particle formation (temperature, humidity) on the basis of statistical relationships and thus atmospheric mechanisms.

The new aspect of this work is the focus on fine particle composition and secondary pollutant characteristics. It is hypothesized that secondary particle composition and fine particle concentrations are influenced by meteorological parameters but PNC of nucleation and Aitken mode as well as mass concentration of fresh emitted particles are driven by emissions mainly. We are aware that the amount of emitted nucleation particles depends on temperature also (see Bukowiecki et al. (2003): formation of primary UFP is enhanced at cold temperatures). Further, the nucleation due to secondary formation processes is strongly dependent on temperature. However, it is not possible on the basis of the measurements used here to differentiate the complex multiphase processes leading to the formation and transformation of SOA in ambient air. For instance it is not possible to differentiate products from homogenous gas-phase oxidation fol-

lowed by condensation of lower volatile products onto SOA from products formed from (heterogeneous) oxidation of condensed or adsorbed compounds in the particle phase (aging). Statistical analyses by real-time correlation of measured data cannot consider the time-lag of these processes which may add to the identified secondary organic compounds of PM. Unfortunately, we did not observe a nucleation event during our measurement period.

Following the introduction in Section 1 Section 2 describes the sites and the instrumentation, Section 3 presents the analysis methods, Section 4 discusses the results and Section 5 presents the conclusions.

2 Measurement methods and data

2.1 Study area

The measurements were performed in Augsburg, Germany, a town with 268,000 inhabitants in 2010 (Stat. Jahrbuch, 2013), and situated in a rural area at the river Lech. The Lech flows northbound perpendicular to the Alps (about 100 km south of Augsburg) towards the Danube in a shallow valley about 10 km wide and 100 m deep. Under synoptically calm conditions with weak pressure gradients, we observed light winds from the South at night and from the North to the Northeast during the day. For stronger large-scale pressure gradients, the winds did not deviate much from the large-scale synoptic winds (Jacobeit, 1986). The prevailing wind direction in such cases was from the Southwest where there are no big emission sources near Augsburg. A number of measurement sites were operated and are described below.

2.2 Urban background site

This site is located on the campus of the Augsburg University of Applied Sciences Hochschule Augsburg (HSA) which is approximately 1 km to the Southeast of the city centre (Fig. S1; Open Street Map, 2013). Within a radius of approximately 200 m, the monitoring site is almost completely surrounded by university and residential areas, apart from a small park located to the Northwest. The nearest main road is to the Northeast at a distance of 120 m and a larger main road with crossing this main road is to the Southeast at a distance of 270 m. HSA was carefully selected as an urban background site by taking into account the representativeness of a single monitoring station for the exposure of the general population to UFP (Cyrys et al., 2008).

The PM composition was measured continuously by an aerosol mass spectrometer (AMS) in the PM_1 range and by an aethalometer (Series 8100, Thermo Fisher Scientific Inc., Franklin, MA, USA), which measured the BC (black carbon) content of $PM_{2.5}$. A high-resolution time-of-flight AMS (Aerodyne Research Inc., Billerica, MA, USA; described in DeCarlo et al., 2006) was used with a collection efficiency of 0.5 for the AMS measurements. Additionally, the fragmentation table (Allan et al., 2004) of the AMS data analysis tools (SQUIRREL v1.49 and PIKA v.1.08, Sueper, 2010) were modified according to the fragmentation table suggested by Aiken et al. (2008). The AMS analysis determined the non-refractory particle components nitrate (NO_3^-), sulphate (SO_4^{2-}), ammonium (NH_4^+), chloride (Cl^-) and organic matter. These measurements and data are described in detail in Elsasser et al. (2012).

PSD were measured by a custom-built particle size spectrometer consisting of twin cylindrical type differential mobility particle sizer, from which PNC in the different size ranges 3–10 (NC3–10), 10–30 (NC10–30), 30–50 (NC30–50), 50–100 (NC50–100), 100–500 nm (NC100–500) were collected. The general set-up of this instrument has been described in detail elsewhere (Birmili et al., 1999). Size-segregated PMC were calculated from PSD data, assuming a spherical shape of particles and a mean particle density of 1.5 g/cm^3 (Pitz et al., 2008). Unfortunately, data in the size ranges 850 nm–10 µm, which are often measured here, are missing. PM_{10} and $PM_{2.5}$ mass concentrations were measured by two tapered element oscillating microbalance/filter dynamics measurement systems (TEOM Model 1400a, Thermo Fisher Scientific Inc., Franklin, MA, USA).

A ceilometer CL31, an eye-safe commercial mini-lidar system, from Vaisala GmbH, Hamburg, Germany, was operated at this station (Münkel, 2007; Münkel et al., 2012). Ceilometers, that were originally developed to monitor the cloud height, can estimate MLH fairly well in the absence of low clouds and precipitation and during scattered clouds. Special software for these ceilometers provides routine retrievals of up to 5 lifted layers, e.g. convective layer depths exceeding 2000 m and nocturnal stable layers down to 50 m, from vertical profiles (vertical gradient) of laser backscatter density data. The structures seen by the ceilometer agreed well with the data profiles measured by radiosonde and derived MLH (location of strong height gradient of laser backscatter density and relative humidity/temperature inversion) as shown by Emeis et al. (2008).

2.3 Air quality monitoring network (LÜB)

Air pollution data from four Bavarian air quality monitoring system Lufthygienisches Landesüberwachungssystem Bayern (LÜB) stations are investigated: Bourgesplatz (urban background), Karlstrasse (urban traffic site), Königsplatz (urban traffic site), and LfU (urban background at the southern edge of the city) (www.lfu.bayern.de/luft/index.htm#a0101). The data include mass concentrations of PM_{10} and $PM_{2.5}$ collected on filter paper by β-absorption (FH62-IR,ESM-Anderson Instruments GmbH, Erlangen, Germany), CO by IR-absorption (APMA-360, Horiba, Leichlingen, Germany), NO and NO_2 by chemiluminescence (APNA-370, Horiba, Leichlingen, Germany), O_3 by UV-absorption (APOA-370, Horiba, Leichlingen, Germany)

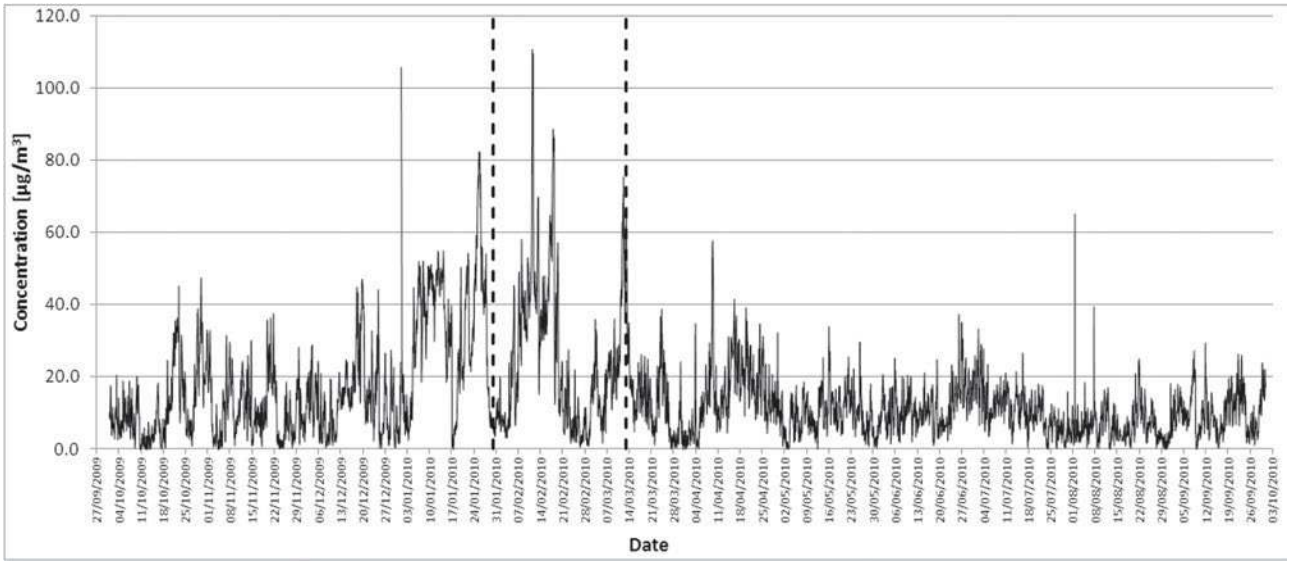

Figure 1: Time series of hourly-mean values of $PM_{2.5}$ mass concentration measurements at the urban background site HSA from 01 October 2009 to 30 September 2010. The measurement period from 0000 CET 31 January to 2400 CET 12 March 2010 is indicated by dashed lines.

as well as benzene, toluene and o-xylene by gaschromatography (GC-U102 BTX, Siemens, Karlsruhe, Germany) measurements.

2.4 Northern edge of the city

Temperature, pressure, relative humidity, wind speed, wind direction, cloud cover, precipitation and sunshine were provided by Germany's National Meteorological Service Deutscher Wetterdienst (DWD) (Weather Request and Distribution System www.dwd.de/webwerdis) station at the Airport Augsburg.

Another site was at the area of the waste treatment plant Abfallverwertungsanlage Augsburg (AVA) which is located at the northern city edge of Augsburg in an industrial area near to the highway A8 and about 2 km south of Augsburg Airport. PM_{10}, NO, NO_2 and O_3 were measured at this site using the same methods described in Section 2.3 and CO is detected precisely by fluorescence measurements (AL5001, Aerolaser GmbH, Garmisch-Partenkirchen, Germany). The vertical profiles of wind, dispersion parameters and temperature up to 500 m were continuously measured during stable or neutral atmospheric conditions by a RASS from Metek GmbH, Elmshorn, Germany. MLH was determined from the inversion of the temperature profiles which are available if the atmosphere is not well-mixed as during the afternoon hours. Also MLH by RASS agreed well with those retrieved by ceilometer (see Emeis et al., 2004, 2008, 2012). In this study, MLH data from ceilometer measurements (Section 2.2) were taken if no RASS results are available. Further, ceilometer MLH was used if the MLH is lower than the cloud lower boundary and if no fog is detected. If this was not the case, the available RASS data were used.

3 Analysis methods

3.1 Selection of analyses period

A one year time series of hourly-mean values of $PM_{2.5}$ mass concentration measurements at the urban background site HSA from 01 October 2009 to 30 September 2010 is shown in Fig. 1. The higher mass concentration level during winter and the hourly $PM_{2.5}$ mass concentration peak (110 µg/m^3 maximum on 11 February 2010) are clearly visible. There were twelve limit value exceedances of PM_{10} with daily-mean mass concentrations up to 96 µg/m^3 at the urban background site LfU during winter (no NO_2 limit value exceedances). High $PM_{2.5}$ mass concentrations during winter and the large number of PM_{10} limit value exceedances motivated to study the period from 0000 CET 31 January to 2400 CET 12 March 2010 in more detail.

3.2 Selection of pollutant data from measurements at different sites

As only chemical composition of PM was measured at the site HSA, it was necessary to take data for all gaseous pollutants from another urban background site. The hourly-mean values of measurement results at the sites Bourgesplatz (LÜB), LfU (LÜB), HSA and AVA are shown in Table 1 as well as Fig. S2 in the supplement. The location of Bourgesplatz is very similar to the site HSA so that NO and NO_x were used from this site (higher NO and NO_x mass concentrations than at AVA and LfU). The other air pollutants were not measured here so that the CO, O_3, benzene, toluene and o-xylene mass concentrations were taken from the site LfU (higher CO and O_3 mass concentrations than at the site AVA). $PM_{2.5}$ and PM_{10} mass concentrations were used from the HSA where all the other particle parameters were measured.

Table 1: Correlation coefficients R^2 of hourly-mean values of NO and NO_x mass concentrations measured at the station Bourgesplatz with LfU and AVA, O_3 and CO mass concentrations measured at the station LfU with AVA as well as $PM_{2.5}$ and PM_{10} mass concentrations measured at the station LfU with HSA. More details are in Fig. S2. No correlations are given if no data are available.

Site	NO	NO_x	O_3	CO	$PM_{2.5}$	PM_{10}
AVA	0.45	0.60	0.88	0.78		
HSA					0.93	0.86
Bourgesplatz	1	1				
LfU	0.54	0.65	1	1	1	1

3.3 Positive Matrix Factorization (PMF) analyses results of particle source contributions used for correlation studies

PMF is a bilinear unmixing model which provides the opportunity to describe e.g. the measured PM composition as a linear combination of factors which represent physically positive mass concentrations. Analysing AMS data a factor contains a constant mass spectrum (factor profile) and a variable contribution with time (factor strength). Normally, these factors are dominated by sources (Lanz et al., 2007; Ulbrich et al., 2009; Paatero and Tappert, 1994; Paatero, 1997).

The PMF analysis for the organic fraction/matter measured by the AMS followed the procedure described by Ulbrich et al. (2009) and is described and discussed in detail in Elsasser et al. (2012). The PMF analysis obtained a three-factor solution performed by FPEAK 0.2 with 14285 time points and 268 mass-to-charge ratios (m/z) from m/z = 12 to 300. In this three-factor solution, the factors freshly emitted HOA – hydrocarbon-like organic aerosol (primary organic factor), which is related to traffic, and WCOA – wood combustion organic aerosol (wood combustion factor) were found. Additionally, one non-source related factor could be calculated for OOA – oxygenated organic aerosol (secondary organic aerosol factor), which is mainly of secondary origin.

The PMF method was also applied to the PSD data to identify possible particle sources by Gu et al. (2011). Since no measurement error was available for PSD, the uncertainties were calculated according to empirical equations as described in Gu et al. (2011). Five different factors were determined and assigned to the following particle sources, given the corresponding maximum size for PNC/PMC in the brackets: nucleation (8 nm/–), fresh traffic (20 nm/–), aged traffic (40 nm/200 nm), stationary combustion (80 nm/300 nm) and secondary aerosol (350 nm/500 nm). The factors long-range dust and resuspended dust are missing as only PSD data in the size range from 3.8 nm to 800 nm were available.

The results of the abovementioned PMF analyses of AMS composition and PSD data are used here. Comparison of source apportionment results from PSD data and from PM_1 composition (see Fig. S3) provides similar sources:

- fresh traffic and aged traffic aerosol factor BC and HOA (traffic factor or primary organic factor),
- stationary combustion aerosol factor BC and WCOA (wood combustion factor),
- secondary aerosol factor OOA (secondary organic aerosol factor).

Further, as shown in Table S1 the secondary aerosol factor is correlated with PM_1, $PM_{2.5}$ and PM_{10}, the stationary combustion aerosol factor with NC100–500, the aged traffic aerosol factor with NC50–100 and NC30–50, the fresh traffic aerosol factor with NC10–30 and the nucleation aerosol factor with NC3–10. These findings correspond to the results in Tables 4 and 5 of Gu et al. (2012).

Finally, the source apportionment provided these main sources: road traffic as well as stationary or wood combustion (see Fig. S3). This is in agreement with the real emissions in the surroundings of the measurement station HSA (see Section 2.2). The mass concentrations of the secondary aerosol are very often higher than these sources. Similar findings are reported by Crippa et al. (2013) for Paris during winter 2010 and also at several sites close and around the Alps (Lanz et al., 2010).

3.4 Definition of different temporal phases

As also done by Birmili et al. (2009) and Crippa et al. (2013), different temporal phases were separated on the basis of hourly-mean, relatively constant values of

- PMC levels (PM_1, $PM_{2.5}$, PM_{10}),
- mass concentrations of organic and inorganic PM components and their relations,
- different PMF factors determined in AMS data analysis,
- weather characteristics (precipitation i.e. wet deposition, wind direction, wind speed and MLH i.e. air mass transport and dilution, temperature as well as relative humidity and absolute humidity i.e. secondary aerosol formation conditions).

These criteria allowed the definition of 10 temporal phases (shown in Figs. 2, 3, S2 and S4 and given quantitatively in Table S2). During the whole study period, the mass concentrations of PM_1, $PM_{2.5}$ and PM_{10} as well as the chemical PM_1 components and PM source contributions varied by more than one order of magnitude. Temperatures and wind speeds ranged from −12 to +13 °C and 0 to 14 m/s, respectively. Unfortunately, phase 4 is one day long only. So the findings about this phase are maybe not substantial.

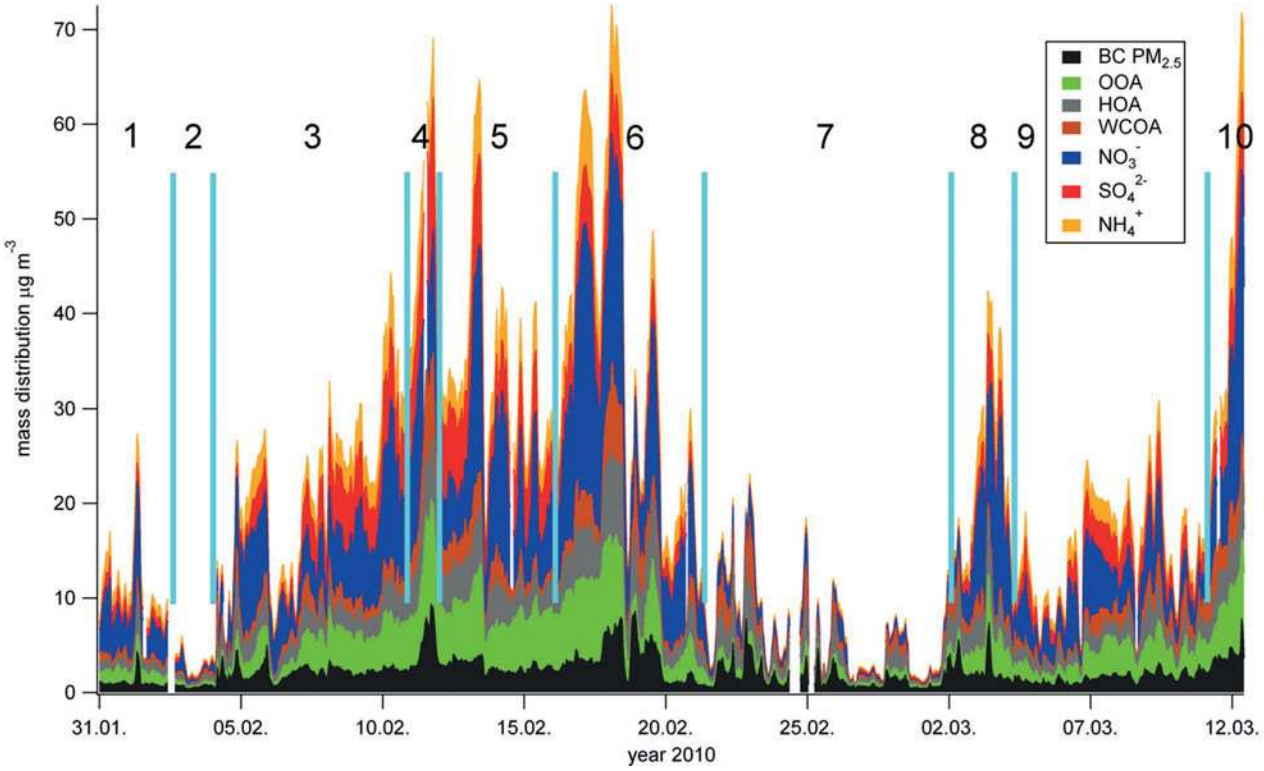

Figure 2: 10 temporal phases of PM_1 fractions (non-refractory particle components and PMF factors) and BC from $PM_{2.5}$ on the basis of hourly-mean values measured at the urban background site HSA (data source from Elsasser et al. (2012)): BC – black carbon, OOA – oxygenated organic aerosol, HOA – hydrocarbon-like organic aerosol, WCOA – wood combustion organic aerosol, NO_3^- – nitrate, SO_4^{2-} – sulphate, and NH_4^+ – ammonium (see text and Table S1). The border of the phases are coloured in light blue.

3.5 Correlations of air pollutant concentrations and PM source contributions with meteorological parameters

Pearson correlation coefficients *r* were calculated between all pollutants and all meteorological parameters using the standardized data (see also Wen and Yeh (2010) and Wu et al. (2013)) on the basis of hourly-mean values (984 data points). Pearson correlation provides the relationship between two variables. Since the variables are measured in different units, utilized standardized data are used for all analyses. The *r*-values, which are numbers between −1 and 1 that determine how much two paired sets of data are related (closer to 1 is more confident), are given in Tables S1 and S3. SO_2 mass concentrations were not considered because the mass concentrations were normally near to the detection limit of the instruments.

Correlation coefficients were then clustered using a hierarchical clustering analysis with the Ward method (Ward, 1963). This is a tool to examine groups of "similar" variables that can be grouped in clusters. The similarity of the variables is examined by the "Ward's minimum variance method". This method aims at finding compact, spherical clusters by examining the variance between cluster members. Heatmaps, including a dendrogram on the columns and rows, help to distinguish the results. The heatmaps presented in all figures are just a color-matrix representation of the Pearson correlation coefficients with the dendrogram obtained after the clustering printed on the margins of the heatmap. Clusters between rows (columns) can be identified by reading the dendrogram from right to left (bottom to top). The length of the branches at each clade represents the similarity between cluster members (e.g., the longer the branch, the greater the difference). The correlation calculations also include the *p*-value for each correlation which is number between 0 and 1 representing the probability that this data would have arisen. A *p*-value of 0.05 is set to show significance. If the correlation results in a *p*-value of less than 0.05, then the study is significant. The hypothesis test to obtain the *p*-values was testing if any correlation exists at all.

Wind polar plots were used where the wind direction is expressed as polar coordinates (circles) and the wind speed by colours. The magnitude is given in the horizontal and vertical axis and corresponds to the standardized values for each pollutant ("standardized" means that all pollutants are forced to have average = 0 and standard deviation = 1 for their data series). The comparisons between pollutants became possible by standardizing the data since this removes the effects of different measuring scales.

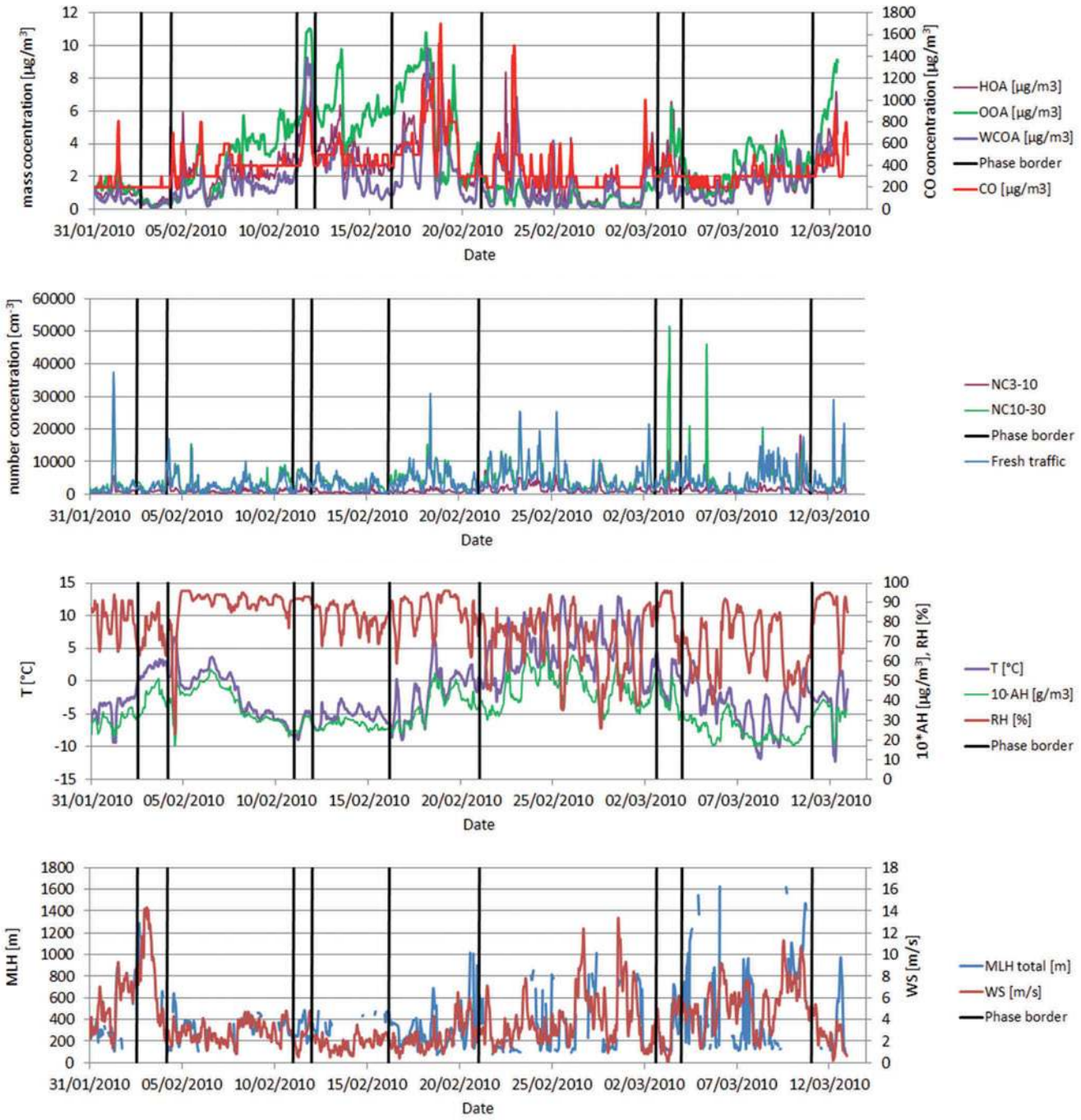

Figure 3: Temporal variation of OOA (oxygenated organic aerosol), HOA (hydrocarbon-like organic aerosol), WCOA (wood combustion organic aerosol) and CO mass concentrations (above), NC3–10, NC10–30 and the fresh traffic aerosol factor (second from above) together with the meteorological parameters T (temperature), RH (relative humidity) and AH (absolute humidity) (third from above) and WS (wind speed) and mixing layer height (MLH) (below). The borders of the 10 phases are drawn too.

4 Results and discussions

4.1 Temporal variations

Fig. 3 shows the temporal variation of PMF factors (HOA, WCOA, OOA and fresh traffic), CO, NC3–10 and NC10–30 together with the meteorological parameters. The wind speed (dilution and transport), humidity (particle growth) and MLH (mixing volume) show a significant influence upon the values of these parameters: low values during high wind speeds/high MLHs/low relative humidity high absolute humidity and high values during low wind speeds/low MLHs high relative humidity/ low absolute humidity. In contrast, the values of NC3–10 (nucleation mode particles), NC10–30 (Aitken mode particles, defined in the size range 10–100 nm), nucleation and fresh traffic aerosol are only weakly dependent on meteorological parameters. This is also shown by all Pearson correlation coefficients in Tables S1 and S3.

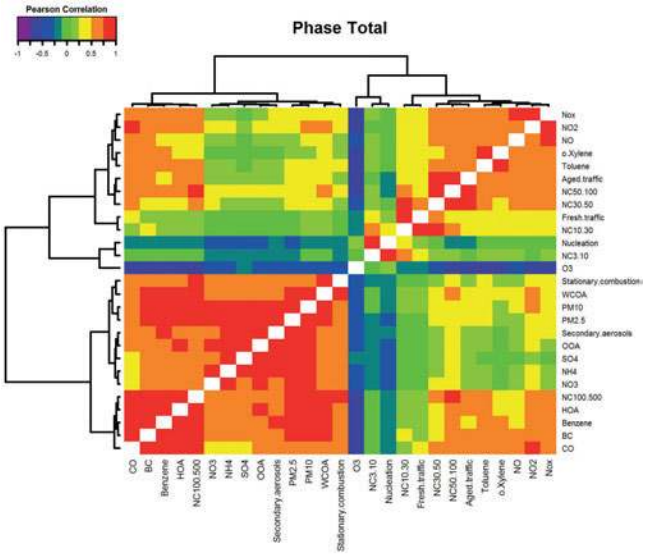

Figure 4: Heatmap with Pearson intercorrelations between all pollutants during the total measurement period (all temporal phases) showing different clusters including the two-dimensional dendrogram on the rows and columns. The correlations are coloured according to the scale on the top-left corner. Correlations between the same variables (equal to 1) are shown in white. Clusters between rows (columns) can be identified by reading the dendrogram from right to left (bottom to top). The length of the branches at each clade represents the similarity between cluster members (e.g., the longer the branch, the greater the difference).

4.2 Correlations of air pollutants, PM components, PM source contributions and PSD modes

Fig. 4 shows a heatmap of the Pearson cross-correlations between all air pollutants (correlations equal to 1 are coloured in white), including dendrograms for rows and columns (obtained with hierarchical clustering), during the total measurement period. Heatmaps with Pearson intercorrelations between all pollutants during all 10 measurement periods are given in Fig. S4. These presentations are "diagonally symmetric" that means what is shown on the top-diagonal is the same as in the low-diagonal. Roughly five clusters with high correlation coefficients can be identified from the heatmap in Fig. 4 by visual inspection, 1) CO, BC, benzene, HOA and NC100–500, 2) $PM_{2.5}$, PM_{10}, NO_3^-, SO_4^{2-}, NH_4^+, OOA, WCOA, secondary aerosol and stationary combustion aerosol, 3) NC10–30 and fresh traffic, 4) NC30–50, NC50–100 and aged traffic, 5) NO, NO_2, NO_x, o-xylene and toluene. There are no strong correlations of NO, NO_2 or NO_x with NO_3^-. As expected, O_3 as secondary gaseous compound shows negative correlations with all pollutants. NC3–10 is only strong correlated with nucleation particles. Note that of all 5 clusters, pollutants in cluster 3, 4 and 5 have r-values mostly lower than 0.8 while in cluster 1 and 2, most strong correlations are found ($r > 0.8$). According to the pollutant types, we consider cluster 1) CO, BC, benzene, HOA and NC100–500 best representing primary pollutants and accumulation mode particles and cluster 2) $PM_{2.5}$, PM_{10}, NO_3^-, SO_4^{2-}, NH_4^+, OOA, WCOA, secondary aerosol, and stationary combustion aerosol best representing fine particles and secondary PM compounds.

4.3 Correlations of air pollutants and meteorological parameters

The results of hierarchical clustering of correlations between pollutants and meteorological parameters during the measurement period (shown in Fig. S5 for each temporal phase and the total period) provide a lot of significant correlations (p-value < 0.05) between pollutants and meteorological parameters (see Table S3). Three groups of phases can be identified from the clustering of correlations with single meteorological parameters (Fig. S5) by comparing the clusters for each meteorological parameter and looking for similarities in the cluster results, considering the frequencies of phases in the clusters, grouping the phases for the meteorological parameters and finalising the grouping by including PMC. The results are shown in Fig. 5 together with phase 4 and the total measurement period, and can be characterised as follows:

1. Very low PMC with high organic content in PM_1. The group 1 shows some peak CO, NO and NO_x mass concentrations, highest temperatures (up to +13 °C), highest wind speeds (up to 14 m/s) and wind directions from west-southwest to south-southeast (influence of university and residential areas). It includes the phases 1, 2, and 7.

2. High PMC with higher organic and SO_4^{2-} content as well as high NO_3^- content in PM_1 mass concentration peaks. Highest CO, NO and NO_x mass concentrations, temperatures mostly below 0 °C and down to −12 °C, low wind speeds (below 7 m/s) and winds from all directions (influence of road traffic) characterize the group 2. Phases 5, 6, and 10 are summarized here.

3. Low to mean PMC with higher NO_3^- content in PM_1. This group has some peak CO, NO and NO_x mass concentrations, temperatures from −12 up to +7 °C, wind speeds between 1 and 11 m/s and wind directions around north (from west-southwest to east, influence of city centre). The phases 3, 8, and 9 are in group 3.

The dendrograms show also that phase 4, the phase of one day and with highest PM pollution during the investigated period, is a special case ("wet" snow fall) which cannot be included in a group: higher WCOA, OOA, HOA and SO_4^{2-} contents as well as high CO, NO and NO_x mass concentrations; temperatures from −9 to −4 °C; lowest wind speeds (0.5 to 5 m/s); wind directions around northwest. The lowest wind speeds during

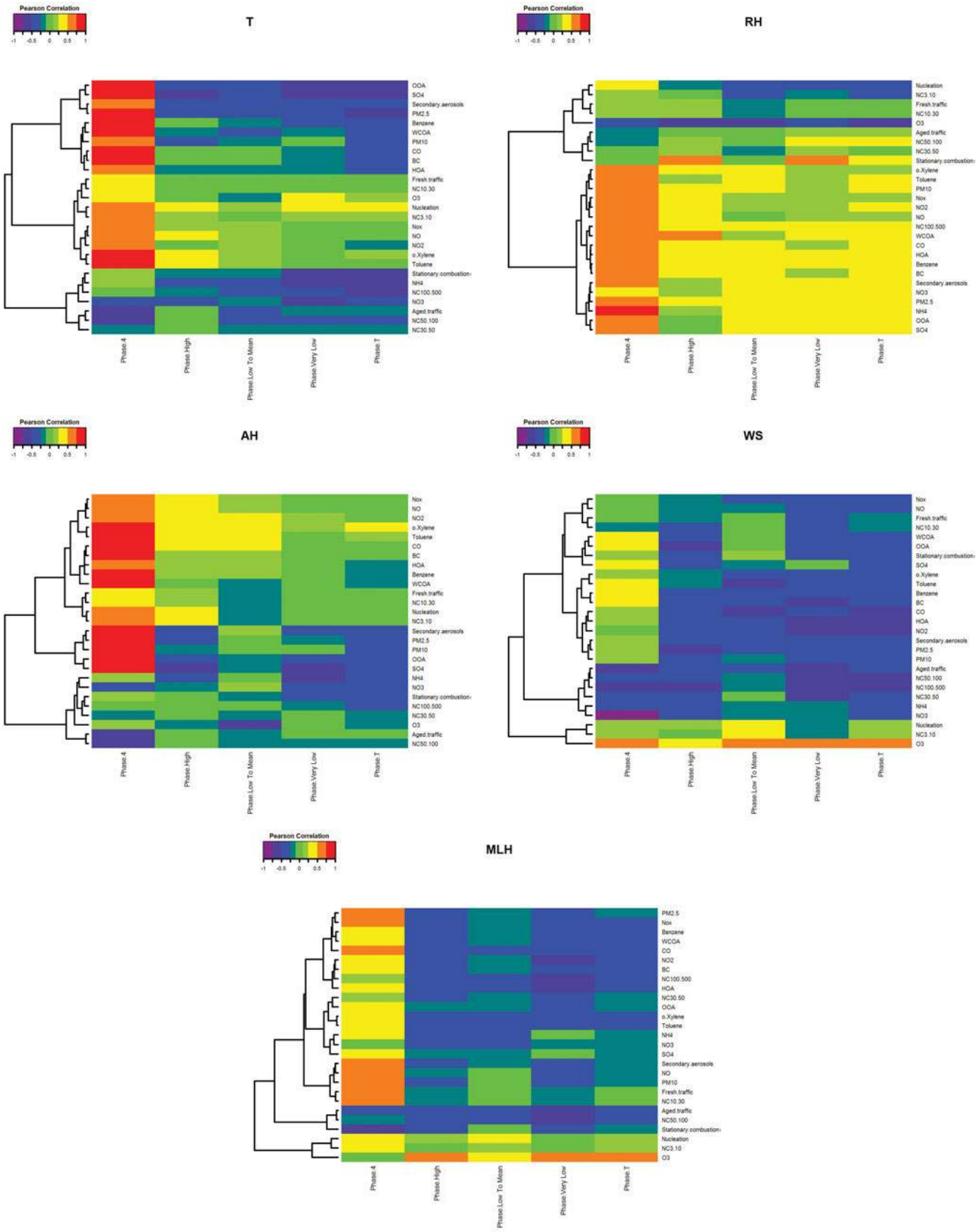

Figure 5: Heatmap with Pearson intercorrelations between pollutants and meteorological parameters (T (temperature), RH (relative humidity), AH (absolute humidity), WS (wind speed), MLH (mixing layer height)) during the measurement period for three groups (phases Very Low, Low To Mean and High concentrations), phase 4 and total period (phase Total) including the dendrogram on the rows. The correlations are coloured according to the scale on the top-left corner. Clusters between rows can be identified by reading the dendrogram from bottom to top. The length of the branches at each clade represents the similarity between cluster members (e.g., the longer the branch, the greater the difference).

the observation period are a dominant influence leading to a strong air pollutant concentration increase and to high concentrations of locally emitted air pollutants. The PM composition provides implications for a relatively high contribution of wood combustion emissions in the surrounding residential areas due to these uncomfortable weather conditions. As the nucleation and Aitken mode particles and the fresh traffic aerosol are only weakly dependent on meteorological parameters these are driven by emissions. High positive correlations of all pollutants (except NO_3^-) with temperature, wind speed, MLH (all these correlations are negative for the other phases) and relative humidity are visible. These findings are maybe not significant due to the short time span of this phase.

There is a similar negative correlation of OOA, secondary aerosol, NO_3^-, SO_4^{2-}, NH_4^+, $PM_{2.5}$, PM_{10} and stationary combustion aerosol (cluster "Secondary PM compounds and fine particles") and NC100–500 with temperature and absolute humidity (Fig. 5). This cluster is more stable during low temperature and thus during low humidity. Primary pollutants like CO, benzene, HOA and BC as well as nucleation mode particles, fresh and aged traffic aerosol, show nearly no dependence on absolute humidity. These pollutants are not chemically transformed or took up water in the atmosphere so that the water vapour concentration has no influence on their concentration.

The concentrations of toluene, NO, NC3–10, NC10–30, NC30–50, nucleation and fresh traffic aerosol, which are only weakly dependent on meteorological parameters, seem to be driven by emissions. This is supported by the fact that the specific PSD in a relatively "clean" air mass does not provide enough particle surfaces for coagulation of UFP which act as a sink for nucleation particles and to a lesser extent for Aitken mode particles.

The signs of the correlations of ozone with meteorological parameters are always opposite to the corresponding sign of all other pollutants as shown in Figs. 5 and S5. This is related to the photochemical formation of ozone (mainly from NO, NO_2 and volatile organic compounds) as well as titration of ozone.

The dependencies of standardized values of concentrations on wind directions and wind speed are shown in Fig. 6. Maximum standardized concentrations are found during wind directions from the Southeast (crossing of two main roads in about 270 m distance), which are characterised by low wind speeds (often wind speed < 1 m/s), for "Primary pollutants" (shown for CO and HOA in Fig. 6) and NO, NO_2, NO_x, o-xylene, toluene, NC30–50 and NC50–100. There is no wind direction dependence for "Secondary PM compounds", NC3–10 and NC10–30. Wind speeds lower than 3 m/s during the events of high concentrations correspond with a low MLH (see Fig. 3).

It is summarized, that wind speed (negative), MLH (negative), relative humidity (positive) and wind direction influence the concentrations of the cluster "Primary pollutants and accumulation mode particles" whereas

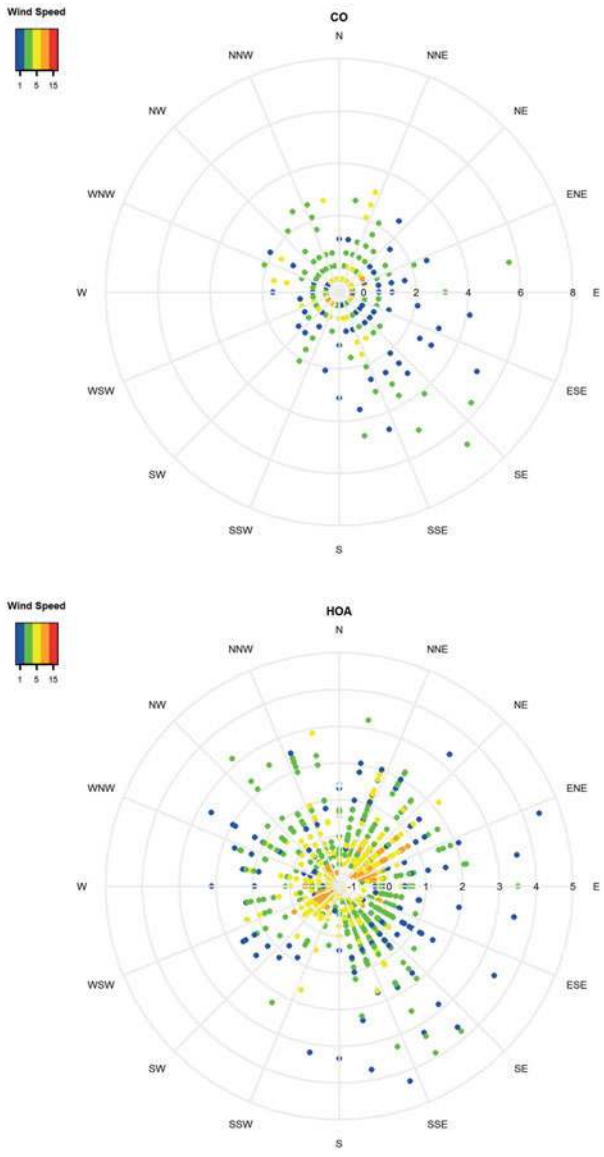

Figure 6: Wind direction, wind speed (top left corner: in different colours, units in m/s) and standardized values of concentration (in different distance to the middle; "standardized" means that all pollutants are forced to have average = 0 and standard deviation = 1 for their data series) plots in polar coordinates for CO and HOA – hydrocarbon-like organic aerosol. Calm wind situations are in blue.

temperature (negative) and absolute humidity (negative) and also relative humidity (positive) influence the cluster "Secondary PM compounds and fine particles".

The comparison of temporal variations of the pollutants during the total measurement period finds that a shift in the concentrations of the pollutants by one or two hours against the meteorological parameters provides higher correlation coefficients and very similar temporal variations. We conclude, that after a change in the weather characteristics, the concentrations of pollutants follow within one to two hours of this weather change (see also Tandon et al., 2010). This time period is required because the air composition of the whole mixing

layer must get the new status by convection or mechanical turbulence if the meteorological parameters change, corresponding to the definition of boundary layer by Stull (1988).

5 Conclusions

The strong temporal variations of gaseous pollutants concentrations, PM composition and PM source contributions are mainly caused by weather changes, because emission variations cannot influence the mass concentrations of gaseous pollutants and PM components to a degree of one order of magnitude during this study period. The results presented here point to a high sensitivity of the

- air pollutant mass concentrations NO_2, CO, benzene, o-xylene, $PM_{2.5}$ and PM_{10},
- PNC of the particle size modes NC50–100 and NC100–500,
- particle component mass concentrations NO_3^-, SO_4^{2-}, NH_4^+ and BC as well as
- mass concentrations of PM source contributions HOA, OOA and WCOA as well as aged traffic, secondary and stationary combustion aerosol

to meteorological parameters. In the sense that a change of climate leads to changes in the frequency and strengths of weather patterns as well as to changes in average and maximum temperature this finding is related to changes in air pollution due to climate change. But climate change has also an impact on emissions from e.g. less heating in winter-time and increased cooling in summer.

New, detailed meteorological influences on air pollutant data, mainly on secondary pollutants and on particle composition, could be found. The different degree of sensitivities to single meteorological parameters is provided by means of correlations of air pollutants, PM components, PM source contributions and PSD modes with all meteorological parameters as well as hierarchical clustering analysis with the Ward method to the correlation coefficients. Generally, wind speed (negatively), MLH (negatively), relative humidity (positively) and wind direction influence primary pollutants and accumulation mode particle (size range 100–500 nm) concentrations; temperature (negatively), absolute humidity (negatively) and also relative humidity (positively) are relevant for secondary compounds of PM and particle ($PM_{2.5}$, PM_{10}) mass concentrations. The dependencies on meteorological parameters are not significant for NO, toluene, NC3–10, NC10–30, NC30–50, nucleation and fresh traffic aerosol. This means that the hypothesis formulated in the introduction, that secondary particle composition, fine particle concentrations and PSD are significant influenced by meteorological parameters, is correct.

The application of general circulation and chemistry transport models, to calculate influences of meteorological parameters, climate change and emission scenarios upon air quality, provide further insight into physical and chemical processes. To get these results a corresponding emission inventory and detailed information about the processes to be simulated are needed. The statistical investigations of meteorological influences upon PM components and gaseous pollutants as shown here provide information in the present atmosphere (see also Tai et al., 2010). Further, the application of various complex statistical methods to analyse measured ambient air data avoids a scaling problem because the measurements shown here are at a point and a model provides results at grids. So, both are necessary and valuable to get a deeper insight: the application of models as well as a thorough investigation of observations.

The results presented here concerning the meteorological influences upon high air pollutant concentrations contribute to general information for aiding epidemiological investigations performed in this urban area (see Cyrys et al., 2008; Gu et al., 2012). Further, this information is necessary for the development of emission reduction measures of certain compounds.

Acknowledgments

We like to thank our colleagues Carsten Jahn, Roman Friedl and Maria Hoffmann (KIT/IMK-IFU) for effective cooperation during the measurement campaign, Christoph Münkel (Vaisala GmbH, Hamburg, Germany) for cooperation within the frame of MLH determination from ceilometer data and Michael Tuma (KIT/IMK-IFU) during his internship for careful MLH analyses from ceilometer and RASS measurements. We are very thankful for the language corrections (both grammar and comprehensibility) of the manuscript by Richard Foreman (KIT/IMK-IFU). We acknowledge support by Deutsche Forschungsgemeinschaft and Open Access Publishing Fund of Karlsruhe Institute of Technology.

References

Aiken, A.C., P.F. DeCarlo, J.-H. Kroll, D.R. Worsnop, J.A. Huffman, K. Docherty, I.M. Ulbrich, C. Mohr, J.R. Kimmel, D. Sueper, Q. Zhang, Y. Sun, A. Trimborn, M. Northway, P.J. Ziemann, M.R. Canagaratna, T.B. Onasch, R. Alfarra, A.S.H. Prévôt, J. Dommen, J. Duplissy, A. Metzger, U. Baltensperger, J.L. Jimenez, 2008: O/C and OM/OC Ratios of Primary, Secondary, and Ambient Organic Aerosols with High Resolution Time-of-Flight Aerosol Mass Spectrometry. – Environ. Sci. Technol. **42**, 4478–4485.

Alföldy, B., J. Osán, Z. Tóth, S. Török, A. Harbusch, C. Jahn, S. Emeis, K. Schäfer, 2007: Aerosol optical depth, aerosol composition and air pollution during summer and winter conditions in Budapest. – Sci. Total Environ. **383**, 141–163.

Allan, J.D., A.E. Delia, H. Coe, K.N. Bower, M.R. Alfarra, J.L. Jimenez, A.M. Middlebrook, F. Drewnick, T.B. Onasch, M.R. Canagaratna, J.T. Jayne, D.R. Worsnop, 2004: A generalised method for the extraction of chemically resolved mass spectra from Aerodyne aerosol mass spectrometer data. – J. Aerosol Sci. **35**, 909–922.

Barmpadimos, I., C. Hueglin, J. Keller, S. Henne, A.S.H. Prévôt, 2011: Influence of meteorology on PM10 trends and variability in Switzerland from 1991 to 2008. – Atmos. Chem. Phys. **11**, 1813–1835.

Barmpadimos, I., J. Keller, D. Oderbolz, D. Hueglin, A.S.H. Prévôt, 2012: One decade of parallel fine (PM2.5) and coarse (PM10–PM2.5) particulate matter measurements in Europe: trends and variability. – Atmos. Chem. Phys. **12**, 3189–3203.

Birmili, W., F. Stratmann, A. Wiedensohler, 1999: Design of a DMA-based size spectrometer for a large particle size range and stable operation. – J. Aerosol Sci. **30**, 549–553.

Birmili, W., K. Weinhold, S. Nordmann, A. Wiedensohler, G. Spindler, K. Müller, H. Herrmann, T. Gnauk, M. Pitz, J. Cyrys, H. Flentje, C. Nickel, T.A.J. Kuhlbusch, G. Löschau, D. Haase, F. Meinhardt, A. Schwerin, L. Ries, K. Wirtz, 2009: Atmospheric aerosol measurements in the German Ultrafine Aerosol Network (GUAN): Part 1 – soot and particle number size distributions. – Gefahrst. Reinhalt. L. **69**, 137–145.

Bukowiecki, N., J. Dommen, A.S.H. Prévôt, E. Weingartner, U. Baltensperger, 2003: Fine and ultrafine particles in the Zürich (Switzerland) area measured with a mobile laboratory: an assessment of the seasonal and regional variation throughout a year. – Atmos. Chem. Phys. **3**, 1477–1494.

Crippa, M., P.F. DeCarlo, J.G. Slowik, C. Mohr, M.F. Heringa, R. Chirico, L. Poulain, F. Freutel, J. Sciare, J. Cozic. C.F. Di Marco, M. Elsasser, J.B. Nicolas, N. Marchand, E. Abidi, A. Wiedensohler, F. Drewnick, J. Schneider, S. Borrmann, E. Nemitz, R. Zimmermann, J.-L. Jaffrezo, A.S.H. Prévôt, U. Baltensperger, 2013: Wintertime aerosol chemical composition and source apportionment of the organic fraction in the metropolitan area of Paris. – Atmos. Chem. Phys. **13**, 961–981.

Cyrys, J., M. Pitz, H. Heinrich, H.E. Wichmann, A. Peters, 2008: Spatial and temporal variation of particle number concentration in Augsburg, Germany. – Sci. Total Environ. **401**, 168–175.

DeCarlo, P.F., J.R. Kimmel, A. Trimborn, M.J. Northway, J.T. Jayne, A.C. Aiken, M. Gonin, K. Fuhrer, T. Horvath, K. Docherty, D.R. Worsnop, J.L. Jimenez, 2006: Field-Deployable, High-Resolution, Time-of-Flight Aerosol Mass Spectrometer. – Anal. Chem. **78**, 8281–8289.

Donateo, A., D. Contini, F. Belosi, A. Gambarano, G. Santachiara, D. Cesari, F. Prodi, 2012: Characterisation of PM2.5 concentrations and turbulent fluxes on a island of the Venice lagoon using high temporal resolution measurements. – Meteorol. Z. **21**, 4, 385–398.

Directive 2008/50/EC, 2008: Directive 2008/50/EC of the European parliament and of the council of 21 May 2008 on ambient air quality and cleaner air for Europe. – Official Journal of the European Union, L 152/2, 11.6.2008.

Elminir, H.K., 2005: Dependence of urban air pollutants on meteorology. – Sci. Total Environ. **350**, 225 – 237.

El-Metwally, M., S.C. Alfaro, 2013: Correlation between meteorological conditions and aerosol characteristics at an East-Mediterranean coastal site. – Atmos. Res. **132–133**, 76–90.

Elsasser, M., M. Crippa, J. Orasche, P.F. DeCarlo, M. Oster, M. Pitz, J. Cyrys, T.L. Gustafson, J.B.C. Pettersson, J. Schnelle-Kreis, A.S.H. Prévôt, R. Zimmermann, 2012: Organic molecular markers and signature from wood combustion particles in winter ambient aerosols: aerosol mass spectrometer (AMS) and high time-resolved GC-MS measurements in Augsburg, Germany. – Atmos. Chem. Phys. **12**, 6113–6128.

Emeis, S., C. Münkel, S. Vogt, W. Müller, K. Schäfer, 2004: Determination of mixing-layer height. – Atmos. Environ. **38**, 273–286.

Emeis, S., K. Schäfer, C. Münkel, 2008: Surface-based remote sending of the mixing-layer height – a review. – Meteorol. Z. **17**, 621–630.

Emeis, S., K. Schäfer, C. Münkel, R. Friedl, P. Suppan, 2012: Evaluation of the interpretation of ceilometer data with RASS and radiosonde data. – Bound-Lay. Meteor. **143**, 25–35.

Gu, J.W., M. Pitz, J. Schnelle-Kreis, J. Diemer, A. Reller, R. Zimmermann, j. Soentgen, M. Stoelzel, H.E. Wichmann, A. Peters, J. Cyrys, 2011: Source apportionment of ambient particles: Comparison of positive matrix factorization analysis applied to particle size distribution and chemical composition data. – Atmos. Environ. **45**, 1849–1857.

Gu, J., M. Pitz, S. Breitner, W. Birmili, S. von Klot, A. Schneider, J. Soentgen, A. Reller, A. Peters, J. Cyrys, 2012: Selection of key ambient particulate variables for epidemiological studies – Applying cluster and heatmap analyses as tools for data reduction. – Sci. Total Environ. **435–436**, 541–550.

Helmis, C.G., G. Sgouros, M. Tombrou, K. Schäfer, C. Münkel, E. Bossiolo, A. Dandou, 2012: A comparative study and evaluation of Mixing Height estimation based on SODAR-RASS, ceilometer data and model simulations. – Bound.-Layer Meteor. **145**, 507–526.

Jacobeit, J., 1986: Stadtklimatologie von Augsburg unter besonderer Berücksichtigung der lufthygienischen Situation sowie des Lärms, Forschungsprojekt im Auftrag und mit Förderung der Stadt Augsburg. – In: Fischer K. (Ed.): Augsburger Geographische Hefte **6**, 171 pp.

Ji, D.S., L. Li, Y.S. Wang, J. Zhang, M.T. Cheng, Y. Sun, Z. Liu, L. Wang, G.Q. Tang, B. Hu, N. Chao, T.X. Wen, H.Y. Miao, 2014: The heaviest particulate air-pollution episodes occurred in northern China in January, 2013: Insights gained from observation. – Atmos. Environ. **92**, 546–556.

Lanz, V.A., M.R. Alfarra, U. Baltensperger, B. Buchmann, C. Hueglin, A.S.H. Prévôt, 2007: Source apportionment of submicron organic aerosols at an urban site by linear unmixing of aerosol mass spectra. – Atmos. Chem. Phys. **7**, 1503–1522.

Lanz, V.A., A.S.H. Prévôt, M.R. Alfarra, S. Weimer, C. Mohr, P.F. DeCarlo, M.F.D. Gianini, C. Hueglin, J. Schneider, O. Favez, B. D'Anna, C. George, U. Baltensperger, 2010: Characterization of aerosol chemical composition with aerosol mass spectrometry in Central Europe: an overview. – Atmos. Chem. Phys. **10**, 10453–10471.

Liu, X., J. Gu, Y. Li, Y. Cheng, Y. Qu, T. Han, J. Wang, H. Tian, J. Chen, Y. Zhang, 2013: Increase of Aerosol Scattering by Hygroscopic Growth: Observation, Modeling, and Implications on Atmospheric Visibility. – Atmos. Res. **132**, 91–101.

Malm, W.C. and D.E. Day, 2001: Estimates of aerosol species scattering characteristics as a function of relative humidity. – Atmos. Environ. **35**, 2845–2860.

Münkel, C., 2007: Mixing height determination with lidar ceilometers – results from Helsinki Testbed. – Meteorol. Z. **16**, 451–459.

Münkel, C., K. Schäfer, S. Emeis, 2012: Confidence levels and error bars for continuous detection of mixing layer heights by ceilometer. – In: Extended Abstracts of Presentations from

the 16th International Symposium for the Advancement of Boundary-Layer Remote Sensing, 5–8 June 2012, Boulder, CO, USA, 98–101.

Open Street Map, 2013: http://www.openstreetmap.org.

Paatero, P., 1997: Least squares formulation of robust non-negative factor analysis. – Chemometr. Intell. Lab. **37**, 23–35.

Paatero, P., U. Tappert, 1994: Positive Matrix Factorization: a non-negative factor model with optimal utilization of error estimated of data values. – Environmetrics **5**, 111–126.

Pal, S., T.R. Lee, S. Phelps, S.F.J. De Wekker, 2014: Impact of atmospheric boundary layer depth variability and wind reversal on the diurnal variability of aerosol concentration at a valley site. – Sci. Total Environ. **496**, 424–434.

Pitz, M., W. Birmili, O. Schmid, A. Peters, H.E. Wichmann, J. Cyrys, 2008: Quality control and quality assurance for particle size distribution measurements at an urban monitoring station in Augsburg, Germany. – J. Environ. Mon. **10**, 1017–1024.

Rost, J., T. Holst, E. Sähn, M. Klingner, K. Anke, D. Ahrens, H. Mayer, 2009:. Variability of PM10 concentrations dependent on meteorological conditions. – Int. J. Environ. Pollut. **36**, 3–18.

Rückerl, R., A. Schneider, S. Breitner, J. Cyrys, A. Peters, 2011: Health Effects of Particulate Air Pollution – A Review of Epidemiological Evidence. – Inhal. Toxicol. **23**, 555–592.

Schäfer, K., S. Emeis, H. Hoffmann, C. Jahn, 2006: Influence of mixing layer height upon air pollution in urban and suburban areas. – Meteorol. Z. **15**, 647–658.

Schäfer, K., S. Emeis, S. Schrader, S. Török, A. Alföldy, J. Osan, M. Pitz, C. Münkel, J. Cyrys, A. Peters, S. Sarigiannis, P. Suppan, 2011: A measurement based analysis of the spatial distribution, temporal variation and chemical composition of particulate matter in Munich and Augsburg. – Meteorol. Z. **21**, 47–57.

Spindler, G., A. Grüner, K. Müller, S. Schlimper, H. Herrmann, 2013: Long-term size-segregated particle (PM10, PM2.5, PM1) characterization study at Melpitz – influence of air mass inflow, weather conditions and season. – J. Atmos. Chem. **70**, 165–195.

Stat. Jahrbuch, 2013: Statistisches Jahrbuch der Stadt Augsburg. – Online available at: http://www.augsburg.de/fileadmin/user_upload/buergerservice_rathaus/rathaus/statisiken_und_geodaten/statistiken/jahrbuch/jahrbuch_2012.pdf.

Stull, R.B., 1988: An Introduction to Boundary Layer Meteorology. – Kluwer Academic Publishers, Dordrecht, Boston, London, 666 pp.

Sueper, D., 2010: ToF-AMS High Resolution Analysis Software – Pika. – online available at: http://cires.colorado.edu/jimenez-group/ToFAMSResources/ToFSoftware/PikaInfo/.

Tai, A.P.K., L.J. Mickley, D.J. Jacob, 2010: Correlations between fine particulate matter (PM2.5) and meteorological variables in the United States: Implications for the sensitivity of PM2.5 to climate change. – Atmos. Environ. **44**, 3976–3984.

Tandon, A., S. Yadav, A.K. Attri, 2010: Coupling between meteorological factors and ambient aerosol load. – Atmos. Environ. **44**, 1237–1243.

Ulbrich, I.M., M.R. Canagaratna, Q. Zhang, D.R. Worsnop, J.L. Jimenez, 2009: Interpretation of organic components from Positive Matrix Factorization of aerosol mass spectrometric data. – Atmos. Chem. Phys. **9**, 2891–2918.

Ward, J.H., 1963: Hierarchical grouping to optimize an objective function. – J. Am. Stat. Assoc. **58**, 236–244.

Wagner, P., 2014: Analyse von biogenem und anthropogenem Isopren und seiner Bedeutung als Ozonvorläufersubstanz in der Stadtatmosphäre. – Inaugural-Dissertation zur Erlangung des Doktorgrades Dr. rer. nat. der Fakultät für Biologie an der Universität Duisburg-Essen, 142 pp.

Wen, C.-C. and H.-H. Yeh, 2010: Comparative influences of airborne pollutants and meteorological parameters on atmospheric visibility and turbidity. – Atmos. Res. **96**, 496–509.

Wu, S., F. Deng, X. Wang, H. Wei, M. Shima, J. Huang, H. Lu, Y. Hao, C. Zheng, Y. Qin, X. Lu, X. Guo, 2013: Association of Lung Function in A Panel of Young Healthy Adults with Various Chemical Components of Ambient Fine Particulate Air Pollution in Beijing, China. – Atmos. Environ. **77**, 873–884.

Xu, W.Y., C.S. Zhao, L. Ran, Z.Z. Deng, P.F. Liu, N. Ma, W.L. Lin, X.B. Xu, P. Yan, X. He, J. Yu, W.D. Liang, L.L. Chen, 2011: Characteristics of pollutants and their correlation to meteorological conditions at a suburban site in the North China Plain. – Atmos. Chem. Phys., **11**, 4353–4369, 2011.

Yue, D., M. Hu, Z. Wu, Z. Wang, S. Guo, B. Wehner, A. Nowak, P. Achtert, A. Wiedensohler, J. Jung, Y.J. Kim, S. Liu, 2009: Characteristics of aerosol size distributions and new particle formation in the summer in Beijing. – J. Geophys. Res. **114**, D00G12. DOI:10.1029/2008jd010894.

Zhang, Q.H., J.P. Zhang, H.W. Xue, 2010: The challenge of improving visibility in Beijing. – Atmos. Chem. Phys. **10**, 7821–7827.

Zhao, P., X. Zhang, X. Xu, X. Zhao, 2011: Long-term visibility trends and characteristics in the region of Beijing, Tianjin, and Hebei, China. – Atmos. Res. **101**, 711–718.

The pdf version (Adobe Java Script must be enabled) of this paper includes an electronic supplement:
Table of content

Tables S1, S2, S3
Figures S1, S2, S3, S4, S5